the plant journal

SEB Society for Experimental Biology

The Plant Journal (2018) **94,** 192–202 doi: 10.1111/tpj.13848

TECHNICAL ADVANCE

Cellular distribution of secretory pathway markers in the haploid synergid cells of *Arabidopsis thaliana*

Daniel S. Jones[1], Xunliang Liu[2], Andrew C. Willoughby[1], Benjamin E. Smith[3], Ravishankar Palanivelu[2] and Sharon A. Kessler[4,5,*]

[1]*Department of Microbiology and Plant Biology, The University of Oklahoma, Norman, OK 73069, USA,*
[2]*School of Plant Sciences, University of Arizona, Tucson, Arizona 85721, USA,*
[3]*Vision Sciences, University of California, Berkeley, CA 94720, USA,*
[4]*Department of Botany and Plant Pathology, Purdue University, West Lafayette, IN 47907, USA, and*
[5]*Center for Plant Biology, Purdue University, West Lafayette, IN 47907, USA*

Received 11 October 2017; revised 21 December 2017; accepted 17 January 2018; published online 31 January 2018.
*For correspondence (e-mail sakessler@purdue.edu).

SUMMARY

In flowering plants, cell–cell communication plays a key role in reproductive success, as both pollination and fertilization require pathways that regulate interactions between many different cell types. Some of the most critical of these interactions are those between the pollen tube (PT) and the embryo sac, which ensure the delivery of sperm cells required for double fertilization. Synergid cells function to attract the PT through secretion of small peptides and in PT reception via membrane-bound proteins associated with the endomembrane system and the cell surface. While many synergid-expressed components regulating PT attraction and reception have been identified, few tools exist to study the localization of membrane-bound proteins and the components of the endomembrane system in this cell type. In this study, we describe the localization and distribution of seven fluorescent markers that labelled components of the secretory pathway in synergid cells of *Arabidopsis thaliana*. These markers were used in co-localization experiments to investigate the subcellular distribution of the two PT reception components LORELEI, a GPI-anchored surface protein, and NORTIA, a MILDEW RESISTANCE LOCUS O protein, both found within the endomembrane system of the synergid cell. These secretory markers are useful tools for both reproductive and cell biologists, enabling the analysis of membrane-associated trafficking within a haploid cell actively involved in polar transport.

Keywords: *Arabidopsis thaliana*, embryo sac, endomembrane system, female gametophyte, LORELEI, MLO, NORTIA, pollen tube reception, pollination, synergid.

INTRODUCTION

Sexual reproduction in flowering plants requires communication between highly specialized cells to ensure the successful delivery, reception, and fusion of gametes (Russell, 1992; Chevalier *et al.*, 2011). This need for cell–cell communication is primarily due to the complex nature of their reproductive development. Multicellular gametophytes (the gamete-producing generation) of flowering plants develop deep within the tissues of entirely separate floral organs (male gametophytes in anthers and female gametophytes in ovules) (Tucker and Koltunow, 2014; Hafidh *et al.*, 2016). In order to reproduce, the male gametophyte (pollen) must land on a receptive stigma of a flower and produce a tip-elongating pollen tube (PT) to transport the male gamete(s) through the pistil to the female gametophyte (embryo sac). The mature pollen grain of *Arabidopsis thaliana* is tricellular, made up of two sperm cells and a vegetative cell, while the mature embryo sac is composed of seven cells [the egg cell and central cell (the two female gametes)], along with five accessory cells consisting of two synergids and three antipodals (Figure 1a; Drews and Yadegari, 2002). The two synergids are located at the micropylar end of the embryo sac and have critical roles in

mediating both the attraction and reception of the PT. Synergids secrete small cysteine-rich peptides (LUREs) that attract the PT and guide its growth towards the ovule micropyle (Higashiyama and Takeuchi, 2015). After arriving and communicating with the receptive synergid cell, PT reception initiates as the PT pauses its growth. The PT then enters the embryo sac and ruptures, releasing the two sperm cells required for double fertilization (Kessler and Grossniklaus, 2011; Beale and Johnson, 2013). These complex and dynamic interactions have made it difficult to understand the cellular processes occurring in the synergid cells, regulating both PT attraction and reception.

The synergid cell is highly polarized with a large vacuole at one end and a region of extensive membrane invaginations and cell wall in-growths in the micropylar end, known as the filiform apparatus (FA; Mansfield *et al.*, 1991; Huang and Russell, 1992). This region of invagination greatly increases the surface area of the synergid's plasma membrane at the micropylar interface and gives 'transfer cell'-like qualities to the synergid cells (Jensen, 1965; Gunning and Pate, 1969; Sumner and Caeseele, 1989; Mansfield *et al.*, 1991; Huang and Russell, 1992). The FA is the first site of contact between the PT and embryo sac and, although the structure and morphology of the FA differs across taxa, conservation of the FA's positioning at the entrance of the embryo sac suggests that this site is important for communication with the PT upon arrival (Mansfield *et al.*, 1991; Leshem *et al.*, 2013). Additionally, many proteins involved in regulating both attraction and reception of the PT localize to the FA. The cysteine-rich LURE peptides localize to the FA within synergids of both *Torenia fournieri* and *A. thaliana* (Okuda *et al.*, 2009; Takeuchi and Higashiyama, 2012). LUREs are also detected throughout the ovule integument cells surrounding the micropyle, demonstrating that they are actively secreted from the FA into the apoplast of the micropyle (Takeuchi and Higashiyama, 2012). The receptor-like kinase FERONIA (FER), and the glycosylphosphatidylinositol (GPI)-anchored surface protein LORELEI (LRE) both polarly localize to the FA of the synergid cell (Figure 1b), where they function in PT reception (Escobar-Restrepo *et al.*, 2007; Lindner *et al.*, 2015; Liu *et al.*, 2016). FER's localization to the FA is, at least partially, dependent on LRE-mediated chaperoning from the endoplasmic reticulum (ER) and LRE/FER may function together in this pathway as a complex (Li *et al.*, 2015; Liu *et al.*, 2016). The MILDEW RESISTANCE LOCUS O (MLO) family protein NORTIA (NTA), a seven-spanning transmembrane protein also involved in mediating PT reception, initially localizes to Golgi distributed throughout the synergid cell in a mature embryo sac (Figure 1c) and redistributes to the FA in a FER-dependent manner after PT arrival (Kessler *et al.*, 2010; Jones *et al.*, 2017). In a recent structure–function analysis of NTA's role in PT reception, it was found that closely related MLO proteins could substitute for NTA in this pathway if they localized to the Golgi, suggesting that MLO localization in Golgi prior to PT arrival is a pre-requisite for their function in PT reception (Jones *et al.*, 2017).

Proteins localized in the plasma membrane of plant cells mediate communication between multiple cells within a tissue as well as between a cell and its environment. These proteins are targeted to the plasma membrane from within the cell via the secretory pathway. Polar trafficking, the directional transport of proteins to the plasma membrane, utilizes the endomembrane system to recycle proteins and restrict their diffusion within a specific region of the plasma membrane, ensuring a polarized distribution (Naramoto, 2017). Both polarized trafficking and secretion

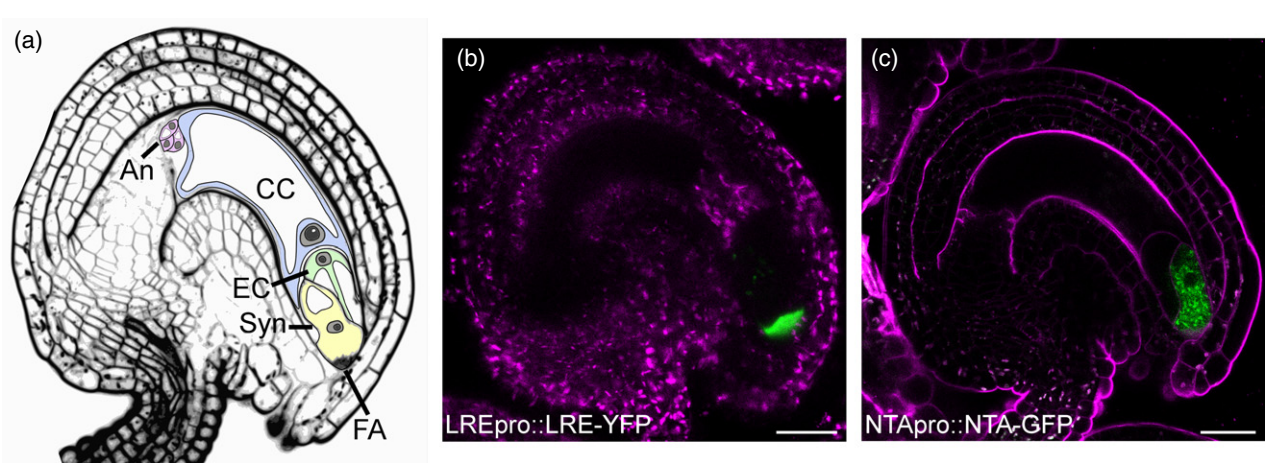

Figure 1. LORELEI and NORTIA expression in the synergid cell.
(a) Diagram of a mature *Arabidopsis thaliana* embryo sac. An, antipodals; CC, central cell; EC, egg cell; FA, filiform apparatus; Syn, synergid.
(b, c) Both LRE and NTA are expressed specifically in the synergid cells of the mature embryo sac. (b) LRE–cYFP (green) in an unpollinated ovule (autofluorescence – magenta). (c) NTA–GFP (green) in an unpollinated ovule labelled with FM4-64 (magenta). Scale bars represent 20 μm.

are involved in PT attraction and reception indicating that the synergid secretory pathway plays a critical role in regulating these processes. Characterizing the secretory pathway in the synergid cell and identifying compartments directly involved in either PT attraction or reception will be a vital step towards understanding key regulatory mechanisms in flowering plant reproduction.

While subcellular markers have been used to describe the localization of both LRE and NTA, both experiments also revealed fluorescent signals beyond the organelle markers used (Liu *et al.*, 2016; Jones *et al.*, 2017). In this study, we used confocal laser scanning microscopy (CLSM) to perform co-localization experiments in the synergid cell with a set of fluorescent markers to label components of the secretory pathway in an attempt to more thoroughly define the distributions of LRE and NTA in the synergid cell before PT arrival. We generated markers based on established proteins or signals (signal peptides and/or retention motifs) that have been shown to localize fluorescent proteins to specific compartments within the endomembrane system of vegetative cells (Nelson *et al.*, 2007; Foresti and Denecke, 2008; Geldner *et al.*, 2009; Drakakaki and Dandekar, 2013). These markers enabled co-localization analyses with known components involved in PT reception and provide a baseline for understanding endomembrane compartment distribution within synergid cells *in vivo* using CLSM. This suite of markers was stably transformed into the Columbia-0 (Col-0) ecotype and characterized in a wild type background (i.e. solely expressed in synergid cells and not in conjunction with other reporter fusion proteins), so that it can serve as a tool to study the secretory pathway of synergid cells by reproductive and cell biology communities.

RESULTS

Distribution of secretory pathway markers in synergid cells

Synergids are specialized cells that function in PT attraction and reception, both processes that require the complex regulation of their secretory pathway for trafficking of cargo. While the biological function of these cells has become clearer, comprehensive analysis of the cellular components directly involved in these processes remains difficult. To bridge this knowledge gap and better describe the secretory pathway of the synergid cell, seven fluorescent markers that localize to different components of the secretory pathway in vegetative cells were expressed under synergid-selective promoters and stably transformed into the Col-0 background (Figure 2 and Table S1). Synergid-expressed markers for the ER, Golgi, peroxisomes and the trans-Golgi Network (TGN; SYP61) had all previously been used in co-localization analyses with LRE and NTA (Liu *et al.*, 2016; Jones *et al.*, 2017), however none of these markers had been solely expressed in synergid cells to determine marker distribution in the absence of other reporter fusion proteins that could adversely affect organelle marker localization. No discernible differences were detected in marker distribution in the wild type background (Figure 2b–d, h) compared with the previous findings (Liu *et al.*, 2016; Jones *et al.*, 2017), indicating that these markers are not noticeably influenced by the presence of either LRE or NTA-reporter fusion proteins.

SP–mCherry–HDEL (an ER-associated marker (Nelson *et al.*, 2007; Liu *et al.*, 2016)) was distributed throughout the synergid cell but was predominantly excluded from the FA (Figure 2b). The reticulate nature of the ER was apparent using this marker in synergids, with transvacuolar strands detected in the chalazal vacuole and a perinuclear envelope observed in all cells imaged. Both the Golgi-associated marker Man49–mCherry (Nelson *et al.*, 2007; Liu *et al.*, 2016) and the TGN-associated markers SYP61 and VHA-a1 (Sanderfoot *et al.*, 2001; Dettmer *et al.*, 2006; Jones *et al.*, 2017) were present in punctate compartments throughout the synergid cell (Figure 2c–e), as previously noted (Liu *et al.*, 2016; Jones *et al.*, 2017). Man49 was never detected in the FA nor was there any polarly distributed signal towards this region of the synergid cells. This localization pattern was markedly different from SYP61 and VHA-a1, which both exhibited two types of distribution. The first type had a signal in the FA (as well as in compartments throughout the cell), while the other only accumulated in punctate compartments and was predominantly excluded from the FA (Figure 2d, d′ and Table S2). RabA1g, which localizes to recycling endosomes in vegetative cells (Rutherford and Moore, 2002; Geldner *et al.*, 2009), was distributed throughout the synergid cell with both diffuse signal and punctate compartmentalization (Figure 2f). Focal accumulations of this marker occurred around the FA, but not necessarily within it. We additionally examined Exo70E2, a subunit of the exocyst complex, that localizes to exocyst-positive organelles (EXPOs) involved in unconventional protein secretion pathways (Wang *et al.*, 2010; Ding *et al.*, 2014). EXPOs have been implicated in both pathogen response and in pollen–stigma interactions during both self-incompatible and compatible pollination in *Brassica* and are, therefore, good candidates for playing a role in synergid function (Samuel *et al.*, 2009; Ding *et al.*, 2012). Exo70E2 varied in its distribution within the synergid cell as was observed with SYP61 and VHA-a1. Punctate compartmentalization of Exo70E2–mCherry was regularly observed and at least some signal was polarly distributed towards the FA (Figure 2g). The majority of synergids imaged had Exo70E2 within the FA, however a few synergids differed with a signal in a line at the top edge of the FA and not within the FA (see Figure 3h). The synergids that differed typically had much larger accumulation of the marker, which also

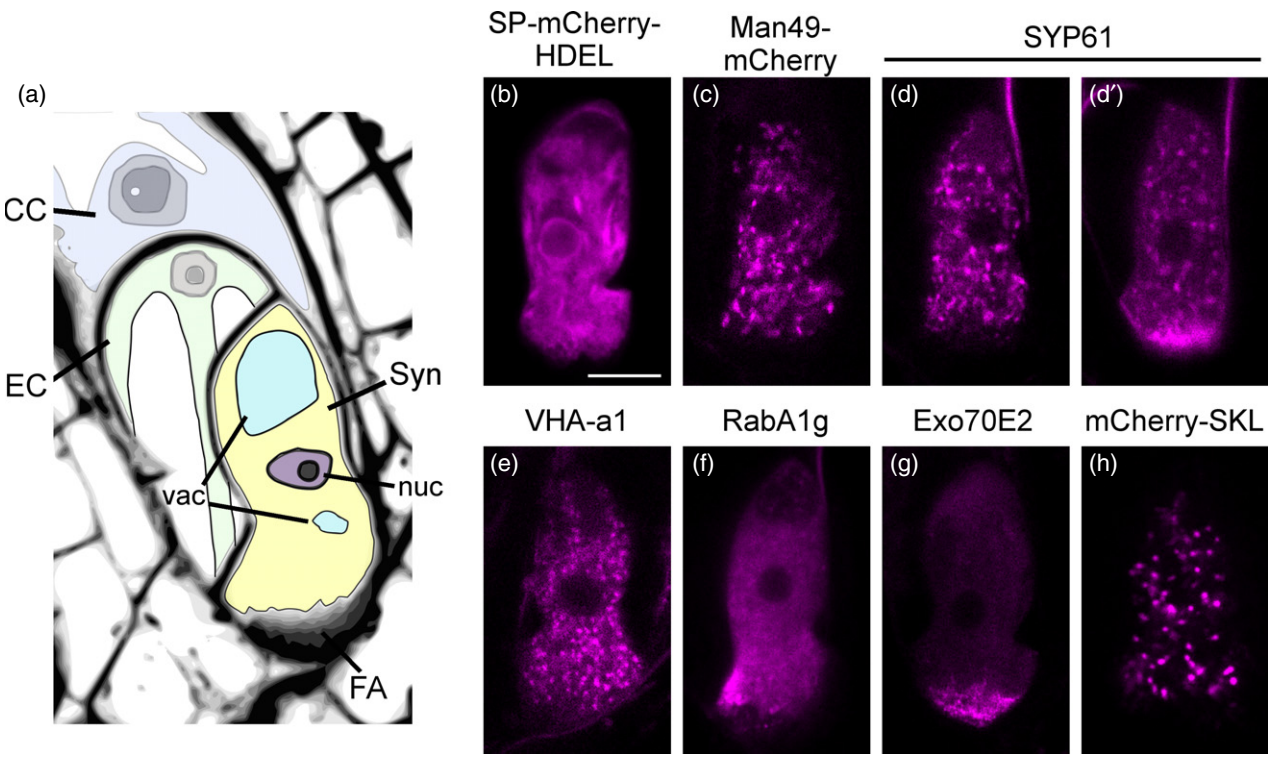

Figure 2. Secretory marker distribution in Col-0 synergids.
Localization of secretory markers (magenta) in synergids of Col-0 from emasculated flowers.
(a) Diagram of a synergid cell at the micropyle of a mature embryo sac. CC, central cell; EC, egg cell; FA, filiform apparatus; nuc, nucleus; Syn, synergid; vac, vacuoles.
(b) Endoplasmic reticulum (ER) – SP–mCherry–HDEL.
(c) Golgi – Man49–mCherry.
(d, e) TGN-associated markers. Both punctate distribution throughout the cell (d) and enrichment towards the filiform apparatus (d′) were commonly observed in both TGN-associated markers: (d) SYP61–mCherry, (e) VHA-a1–mCherry.
(f) mCherry–RabA1g (recycling endosome).
(g) Exo70E2–mCherry [exocyst-positive organelle (EXPO)].
(h) Peroxisome – mCherry–SKL. Bar = 10 μm.

aggregated. These aggregates had a stronger fluorescence signal and thus could be associated with synergids that had higher expression levels of the marker. The peroxisome-associated marker mCherry–SKL (Nelson *et al.*, 2007; Liu *et al.*, 2016) accumulated within spherical compartments that were distributed throughout the synergid cell cytosol, but were excluded from the FA (Figure 2h).

LORELEI partially co-localizes with both SYP61 and VHA-a1 in the filiform apparatus

In unfertilized embryo sacs, LRE primarily accumulates in the FA of the synergid cells; however, LRE also localizes within intracellular compartments distributed throughout the cell (Figure 1b) (Capron *et al.*, 2008; Tsukamoto *et al.*, 2010; Liu *et al.*, 2016). Previous co-localization analyses in synergid cells found that LRE did not overlap with markers associated with the ER, Golgi or peroxisomes (Liu *et al.*, 2016). To determine the identity of these intracellular compartments, a translational fusion of LRE and citrine yellow fluorescent protein (cYFP) was co-expressed with fluorescent markers to label additional components of the secretory pathway in the synergid cell. The four fluorescent markers SYP61, VHA-a1, RabA1g, and Exo70E2 fused to mCherry were co-expressed with LRE–cYFP in synergid cells (Figure 3 and Table S3). These proteins have all been shown to localize to a number of endomembrane-associated compartments involved in endocytic and exocytic trafficking of soluble and membrane-bound cargo in vegetative cells (Foresti and Denecke, 2008; Geldner *et al.*, 2009; Drakakaki and Dandekar, 2013). As LRE–cYFP is highly enriched at the FA, saturation of this signal typically occurs before the LRE-associated intracellular compartments were easily visualized during post-image processing. In order to better analyze these data, images of whole synergids were cropped to remove the FA, enlarged, and the fluorescent signal adjusted to make more informed comparisons between signals corresponding to the YFP and mCherry channels. Overall, no appreciable overlap was observed

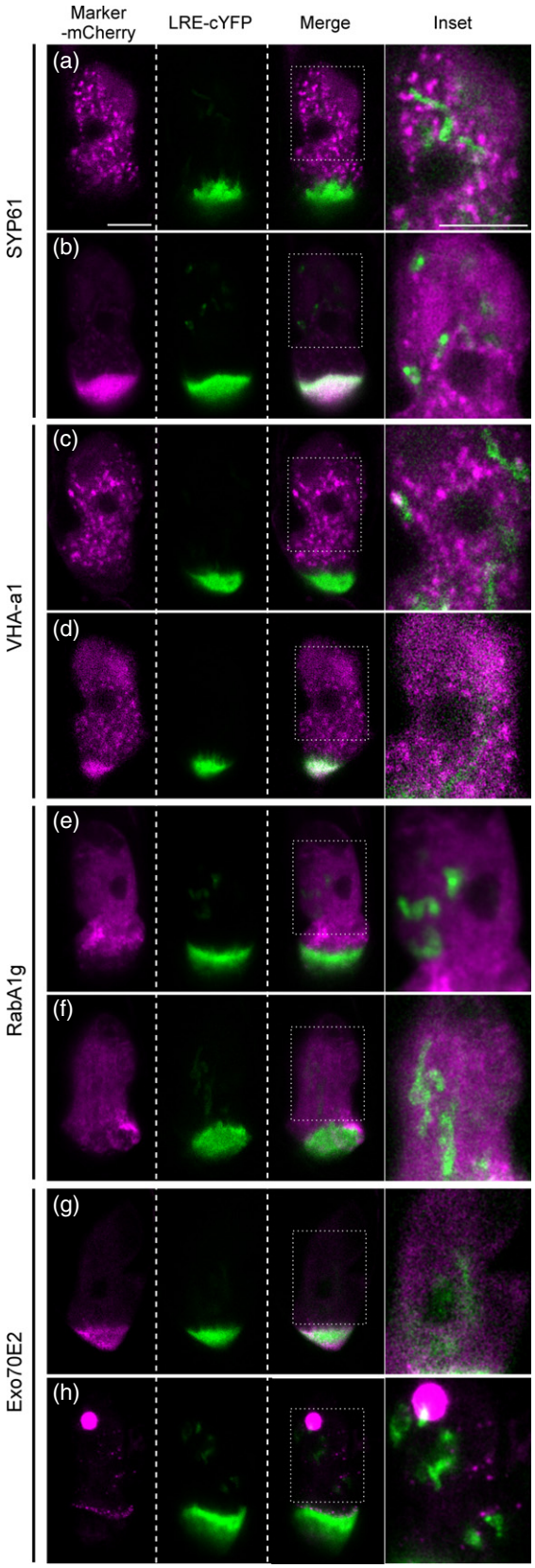

Figure 3. LRE–cYFP co-localization with secretory markers in synergids.
LRE–cYFP (green) co-localization with secretory markers (magenta) in synergid cells of *lre* from emasculated pistils.
(a, b) SYP61–mCherry (TGN-associated).
(c, d) VHA-a1–mCherry (TGN-associated). LRE–cYFP co-localized with both SYP61–mCherry and VHA-a1–mCherry at the filiform apparatus when they were polarly distributed to this region (b, d).
(e, f) mCherry–RabA1g (recycling endosome).
(g, h) Exo70E2–mCherry [exocyst-positive organelle (EXPO)]. Scale bars represent 10 μm. Bar on (a) inset used for all insets.

between LRE-associated intracellular compartments and any of the four markers used in this analysis (Figure 3, insets).

Three markers (SYP61, VHA-a1, and Exo70E2) were distributed towards the FA of synergid cells in a manner similar to or associated with LRE–cYFP (Figure 3). Of the two distribution patterns observed with both SYP61 and VHA-a1, only the signal that accumulated in the FA had any overlap with LRE, indicating that some TGN-associated components may have a role in LRE's distribution to this region (Figure 3b, d). Although the polarly localized Exo70E2 distribution within the FA was similar to LRE–cYFP, the two signals formed distinct subdomains with relatively little overlap (Figure S1). RabA1g was mostly diffuse with some accumulation in punctate compartments throughout the synergid cell and had no detectable overlap with LRE–cYFP (Figure 3e, f). This finding suggests that LRE–cYFP does not co-localize within EXPO-positive compartments and indicates that multiple domains may exist within the FA of *A. thaliana*, an observation made previously about the synergid cells of cotton (*Gossypium hirsutum*) (Jensen, 1965).

Quantitative analysis of NORTIA's co-localization with endomembrane markers in the synergid cell

When expressed from its native promoter, NTA–GFP accumulates specifically in the synergid cells where it mediates PT–synergid communication during PT reception (Figure 1c) (Kessler *et al.*, 2010). NTA–GFP predominantly co-localizes with a Golgi-associated marker in the synergid cell (Jones *et al.*, 2017), however NTA–GFP was also detected in other parts of the synergid cell besides the Golgi, suggesting that it also accumulates within other membrane-bound compartments. The same study found no overlap between the NTA–GFP signal and markers associated with the ER, peroxisomes, or the TGN (SYP61) (Jones *et al.*, 2017). If conventional trafficking pathways mediate NTA–GFP's initial retention within the Golgi or its active redistribution following PT arrival, then these non-Golgi compartments are presumably associated with the secretory pathway and it may be possible to detect overlap between NTA–GFP and the new markers generated in this study. To this end, a translational fusion of NTA–GFP was

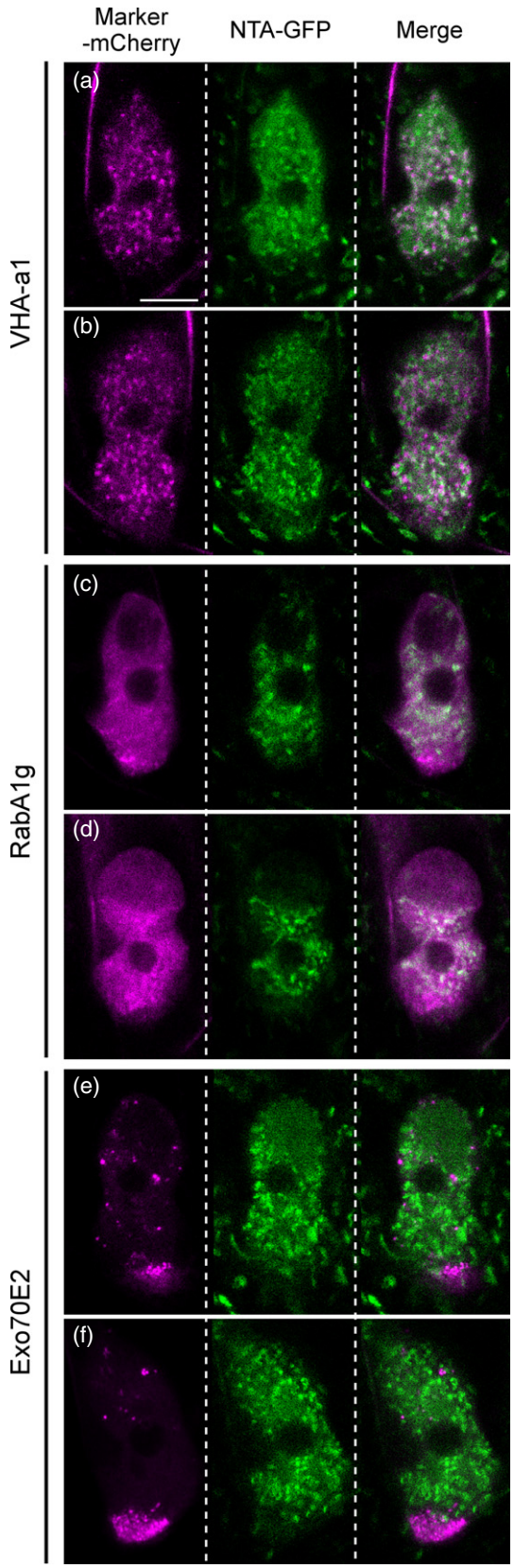

Figure 4. NTA–GFP co-localization with secretory markers in synergids.
NTA–GFP (green) co-localization with secretory markers (magenta) in synergid cells of *nta-1* from emasculated pistils.
(a, b) VHA-a1–mCherry (TGN-associated).
(c, d) mCherry–RabA1g (recycling endosome).
(e, f) Exo70E2–mCherry [exocyst-positive organelle (EXPO)]. Scale bar represents 10 μm.

co-expressed in synergid cells with three additional endomembrane markers that had not previously been co-expressed with NTA (Figure 4 and Table S3).

Co-localization was initially determined qualitatively using merged channels of NTA–GFP and the co-expressed mCherry markers acquired via CLSM. Similar to the NTA–GFP and SYP61–mCherry co-localization pattern previously reported (Jones *et al.*, 2017), no direct overlap was detected between NTA and VHA-a1 (Figure 4a, b), further demonstrating that NTA is probably excluded from TGN-associated compartments prior to PT arrival. However, NTA–GFP and TGN distribution do appear to be closely associated, and agreeing with previous reports that compared Golgi and TGN dynamics using fluorescent markers for each organelle in hypocotyl cells (Viotti *et al.*, 2010). Co-localization of NTA–GFP and mCherry–RabA1g revealed some overlap in merged micrographs, however this overlap was only observed in a portion of the more punctate accumulations of this marker (Figure 4c, d). As RabA1g primarily has a more diffuse distribution within the cell, we cannot say whether there is also overlap with the more diffuse NTA–GFP signal. Due to this situation, there may be some occurrences of co-localization between the two signals that remains below the resolution limits of this system. No overlap was detected for NTA–GFP and Exo70E2–mCherry in unpollinated ovules (Figure 4e, f).

In order to make more direct comparisons between NTA–GFP co-localization with the three markers presented in this study and those previously published, we quantified the degree of co-localization between NTA–GFP and a subset of endomembrane markers analyzed previously that had punctate expression throughout the synergid. NTA–GFP's degree of co-localization with Man49, RabA1g, VHA-a1, SYP61, and mCherry–SKL markers in synergid cells of unpollinated ovules was quantified and compared using both Manders' co-localization coefficients (MCC) and Pearson's correlation coefficients (PCC) (Figure 5) (Manders *et al.*, 1992, 1993). First, in order to enrich for signal coming specifically from vesicles and to suppress instrument noise and background signal, images were processed using a median filter and then a narrow-band spatial bandpass filter (Figure 5b, d, f, h, j; see Experimental Procedures for details). MCC more strictly measures the co-occurrence of the two signals, whereas PCC measures the spatial correlation of the two signals (Dunn *et al.*,

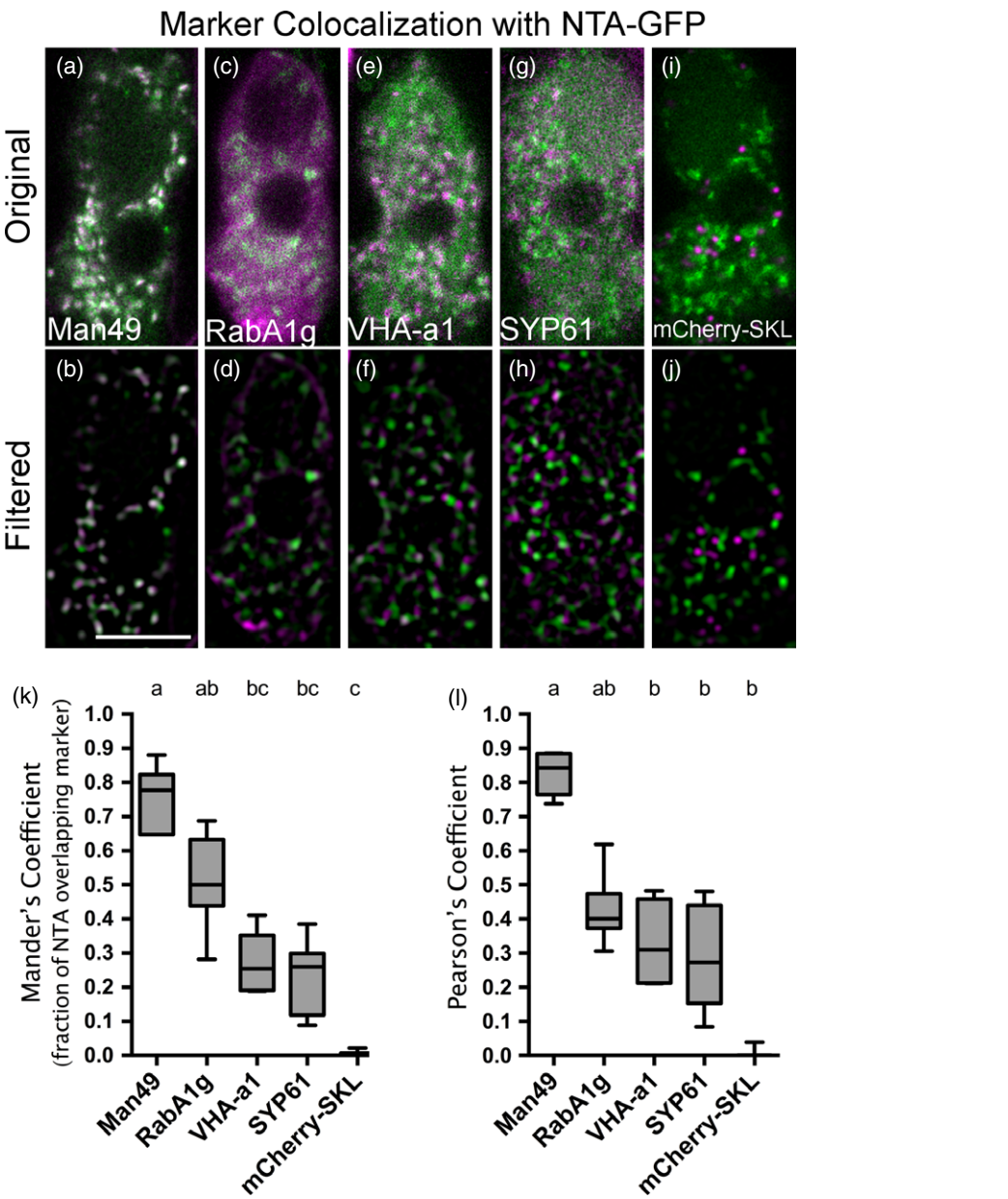

Figure 5. Quantification of NTA–GFP co-localization with markers in synergids.
NTA–GFP (green) co-localization with secretory markers (magenta) that have punctate distributions in synergid cells from emasculated pistils.
(a–j) Original merged image and filtered merged images from: (a, b) NTA–GFP with Man49–mCherry (Golgi-associated marker); (c, d) NTA–GFP with mCherry–RabA1g; (e, f) NTA–GFP with VHA-a1–mCherry; (g, h) NTA–GFP with SYP61–mCherry; and (i, j) NTA–GFP with mCherry–SKL (peroxisome-associated marker).
(k) Comparison of quantification using Manders' co-localization coefficient – only the fraction of NTA–GFP signal overlapping with the marker signal is shown in graph.
(l) Comparison of quantification using Pearson's correlation coefficient. Groupings of (a, b, c) are based on significant differences between datasets determined using the Kruskal–Wallis test. Sample sizes for quantification as follows: NTA + Man49 ($n = 7$), NTA + SYP61 ($n = 6$), NTA + VHA-a1 ($n = 7$), NTA + RabA1g ($n = 8$), NTA + mCherry–SKL ($n = 3$). Scale bar represents 10 μm.

2011). In support of previous findings, both MCC and PCC analyses of NTA–GFP co-localization with Man49 (Golgi) and RabA1g (endosome) showed relatively strong co-localization (Figure 5k, l). Coefficients from NTA co-localization with RabA1g, SYP61, and VHA-a1 were not significantly different from each other with intermediate levels of overlap detected (Figure 5k, l). NTA–GFP and the peroxisome marker had no overlap with a very low overlap coefficient using both metrics (Figure 5k, l). Quantification of NTA's co-localization with these five markers predominantly supports the qualitative interpretation of image data (Figure 4) and Jones *et al.* (2017), as NTA–GFP's

co-occurrence with Man49 (Golgi) is not significantly different from RabA1g (endosome) but is significantly greater than the other markers analyzed.

DISCUSSION

In vivo analysis of the synergid secretory pathway

Ultrastructural and genetic analyses have both provided extensive insight into the biological function of synergid cells from many species (Huang and Russell, 1992; Kessler and Grossniklaus, 2011; Beale and Johnson, 2013). In particular, analyses focusing on PT attraction and reception in the model system *A. thaliana* have produced much of what is known about the complex molecular pathways regulating these critical processes (Kessler and Grossniklaus, 2011; Beale and Johnson, 2013; Higashiyama and Takeuchi, 2015). While the synergid cell's function is dependent on the active secretion of attractant molecules (PT attraction) and the polar distribution of membrane-bound proteins to the FA (PT reception), few tools exist to study the secretory pathway within this cell type *in vivo*. Constitutively expressed markers for secretory pathway compartments have been generated using both the 35S and UBQ10 promoters (Nelson *et al.*, 2007; Geldner *et al.*, 2009). While these marker lines have proven to be extremely useful for sporophytic tissues, their utility in female gametophytes is limited due to the weak expression of the 35S promoter in these cells and the fact that the female gametophyte is buried under several layers of sporophytic tissue, impeding CLSM analysis of these cell types. Highly specific and strong expression of secretory pathway markers in the synergids of *A. thaliana* provides an invaluable tool for the analysis of the cellular processes regulating its function.

The specialized nature of the synergid cell requires a thorough description of the distribution of secretory pathway components in this cell. We found no discernible differences in the distributions of the seven secretory markers assayed when co-expressed with fluorescently labelled PT reception components (LRE and NTA) or when expressed independently. These data suggest that this suite of secretory markers can be used as effective tools for co-localization analyses of synergid-expressed proteins. Additionally, these markers enable the comparative analysis of endomembrane distribution between wild type and more complex genetic backgrounds, such as mutants for essential components involved in regulating the secretory pathway. With many parallels drawn between cell–cell communication during sexual reproduction and responses to pathogens, tools like these markers could demonstrate more similarities between conserved intracellular communication pathways. This situation is especially true when comparing reproductive signaling to defence responses as much is known about the role of the secretory pathway in response to fungal pathogen infection in plants (Hückelhoven and Panstruga, 2011). Investigation of the synergid secretory pathway in PT reception deficient mutants would allow us to explore additional levels of conservation between these two systems. However, the benefits of comparative analyses in synergid cells go beyond understanding the function of synergid-regulated processes. As gametophytic cells, synergids are haploid, enabling the analysis of loss-of-function and dominant-negative mutations that are lethal or have deleterious effects on normal plant growth and development by studying them in a heterozygous background.

While the majority of secretory markers used in this study maintained predictable distribution patterns in synergid cells when compared with previous descriptions (Sanderfoot *et al.*, 2001; Geldner *et al.*, 2003, 2009; Dettmer *et al.*, 2006; Nelson *et al.*, 2007), there was some variation in marker distribution in our analysis. Both SYP61 and VHA-a1 (TGN-associated) varied in their distribution in synergid cells between exclusion from the FA and incorporation in the FA (Table S2). Individuals exhibited consistent distribution of these two fluorescent reporters, with little to no variation between synergids within a single flower. Although the cause of these different distributions is not immediately clear, they were observed across many independent transgenic lines with different levels of marker accumulation, suggesting that it is not an artifact of insertion bias of the transgene. Both SYP61 and VHA-a1 are full-length proteins whose localization had not been previously characterized in gametophytic cells and may be influenced by other components within the cell. While every flower analyzed was imaged 2 days after emasculation (see Experimental Procedures), we cannot rule out environmental factors such as time of day or age of a specific synergid cell in influencing the distribution of these markers. As two different markers for the TGN were analyzed, and both showed variation in distribution within the cell, it is likely that this variability is biologically relevant and could represent an unknown switch in the synergid cell's secretory function (i.e. trafficking processes regulating PT attraction vs. reception). We also observed differences in the distribution of RabA1g (recycling endosome-associated) compared with what was previously reported (Geldner *et al.*, 2009). While punctate accumulations were detected, much of the marker's signal was more diffuse (Figure 2f). This may represent differences in expression level between our system and that previously reported or a cellular difference in how synergids sort and regulate this class of proteins. As another indicator of the synergid cell's complexity, multiple domains within the FA were observed in synergids co-expressing LRE and Exo70E2 (Figure S1). Distinct domains within an FA were previously described in cotton as two 'phases' of the synergid FA, a highly organized region with striations and an amorphous region, but no functional significance for these domains is known

(Jensen, 1965). Our analysis reveals that this characteristic may extend to the FA of *A. thaliana* synergid cells.

The role of the synergid endomembrane system in the distribution of pollen tube reception components

LRE primarily localizes to the FA of the synergid and functions with FER to mediate interactions between the PT and synergid cell during PT reception (Capron *et al.*, 2008; Tsukamoto *et al.*, 2010; Li *et al.*, 2015; Lindner *et al.*, 2015). A recent study exploring LRE function and localization within the synergid also demonstrated its accumulation in additional unknown intracellular compartments throughout the cell (Liu *et al.*, 2016). Based on the nature of LRE's polar distribution, and its role in trafficking FER from the ER to the FA, our original hypothesis was that these LRE-associated intracellular compartments were a component of the secretory pathway (Li *et al.*, 2015; Liu *et al.*, 2016). Co-localization analyses using a set of secretory pathway markers expressed in the synergid cell did not reveal the identity of LRE's intracellular compartment; however, this study did provide some evidence for LRE-related trafficking. The overlap between LRE and the TGN-associated markers SYP61 and VHA-a1 at the FA lends support to the notion that LRE's polar distribution is achieved, in some part, through conventional trafficking processes involving transport through the TGN to the plasma membrane. Additionally, while no direct overlap with RabA1g was found, the unique accumulation of this endosome marker at the FA suggests that there could be a relationship with endosome trafficking and FA-localized proteins (Figure 3e, f). The role of endosomal compartments in polar trafficking has been proposed for the recycling of the PIN-FORMED (PIN) auxin efflux proteins at the plasma membrane and it is possible that the polar accumulation of PT reception components in the FA of the synergid cell could be maintained in this way (Geldner *et al.*, 2003; Reyes *et al.*, 2011; Naramoto, 2017). One function of LRE is at the PT–synergid interface, demonstrated by complementation of the *lre* mutant with ectopic expression of LRE in the PT or with LRE fused to the transmembrane domain of FER (which ensured its localization to the FA in the synergid cell without being cleaved) (Liu *et al.*, 2016). As the LRE/FER receptor complex represents an upstream signaling component of the PT reception pathway, it is likely that the polar transport and maintenance of LRE/FER within the FA is critical for this important cellular function in the synergid.

NTA localizes within the Golgi of the synergid cell prior to PT arrival and redistributes towards the FA sometime during PT reception (Kessler *et al.*, 2010; Jones *et al.*, 2017). Localization to the Golgi is conserved among MLO proteins that can functionally substitute for NTA when expressed in this cell type, and may represent an interaction with an unknown component involved in MLO function during PT reception (Jones *et al.*, 2017). Mobilization of MLO proteins to a focused domain in the plasma membrane is conserved across MLO-mediated processes. During powdery mildew infection, barley MLO redistributes to the site of fungal penetration in epidermal cells, suggesting that polarized MLO trafficking is critical for their function (Bhat *et al.*, 2005; Kessler *et al.*, 2010). Quantification of NTA's co-localization revealed partial co-occurrence of NTA–GFP and mCherry–RabA1g prior to PT arrival, suggesting either that NTA's retention within the Golgi or the prevention of its distribution to the FA is dependent on trafficking through endosome-associated compartments (Figure 5k). In plants, endosomal trafficking is primarily associated with either the TGN, for transport/recycling of cargo to the plasma membrane, or multivesicular bodies (pre-vacuolar compartments), for transport related to protein degradation (Reyes *et al.*, 2011). Interestingly, intermediate levels of co-occurrence were detected between NTA–GFP and the TGN-associated markers VHA-a1 and SYP61 in the synergid cell, however these were significantly lower than NTA's co-occurrence with the Golgi-associated marker Man49 (Figure 5k) (Jones *et al.*, 2017). These data support the hypothesis that NTA's presence in endosome-associated compartments is linked to its transport out of the FA (or plasma membrane), preventing its accumulation in this region before PT arrival. This hypothesis is dependent on NTA's exclusion from the TGN. We cannot, however, rule out that NTA may still be trafficked through the TGN, but that its transport is too rapid and dynamic to detect in our *in vivo* assay (Viotti *et al.*, 2010; Jones *et al.*, 2017).

CONCLUSIONS

In summary, the seven secretory markers described in this study provide a tool to investigate the secretory pathway in synergid cells by the reproductive and cell biology communities. Future studies can utilize this set of markers to identify the cellular compartments involved in PT attraction and reception and more thoroughly dissect processes that regulate the secretory pathway of a highly polarized haploid cell.

EXPERIMENTAL PROCEDURES

Cloning and transformation

Secretory marker fusions with mCherry expressed under the *MYB98pro* (VHAa1 and Exo70E2) were generated in a manner similar to the previously published *MYB98pro*::*SYP61–mCherry* construct (Jones *et al.*, 2017). Expression vectors were generated in the pEarlyGate301 backbone using Gibson Assembly (Gibson Assembly Master Mix NEB E2611S) (Gibson *et al.*, 2009). *VHAa1* and *Exo70E2* were amplified with PHUSION High-Fidelity Polymerase (NEB, M0535S) from Col-0 flower cDNA and *MYB98pro* was amplified out of a modified pMDC83 vector that incorporates the *MYB98pro* (Lindner *et al.*, 2015). Fragments were assembled after restriction digests of pEarlyGate301 with *Pac*I (NEB R0547S) and *Bam*HI (NEB R3136S) followed by gel purification. To

generate *LREpro*::*mCherry–RabA1g* construct, the 959 bp *LRE* promoter and *mCherry* coding sequence were amplified from previous described constructs (Liu *et al.*, 2016); *RabA1g* (AT3G15060) genomic sequence (from ATG to TGA) was amplified from Col-0 genomic DNA. These three fragments were then assembled via overlapping PCR, and cloned into a pFGC19 backbone using In-Fusion HD Cloning Plus (Clontech, cat. no. 638909). A flexible linker (Ala-Gly-Ala-Ala-Ala-Ala-Ala-Gly-Ala) (Tian *et al.*, 2004) was placed between the *mCherry* and *RabA1g* sequences. Primers used for cloning are listed in Table S4. Expression vectors containing the secretory markers were transformed into *Agrobacterium tumefaciens* strain GV3101 and transformed into *LREpro*::*LRE–cYFP*, *MYB98pro*::*NTA–GFP*, and Col-0 via the floral-dip method (Bent, 2006). Details of the *LREpro*::*LRE–cYFP* and *MYB98pro*::*NTA–GFP* lines used can be found in their original articles (Lindner *et al.*, 2015; Liu *et al.*, 2016; Jones *et al.*, 2017).

Plant growth and transgenic selections

Arabidopsis thaliana used for imaging was grown at 22°C under long-day conditions (16 h light/8 h dark) in a custom-built grow room. T1 generation plants were planted directly on soil [ProMix Flex supplemented with 40 g MARATHON pesticide and Peter's 20:20:20 (NPK) fertilizer at recommended levels] and cold-stratified in the dark at 4°C for 2 days. Seedlings were sprayed with BASTA herbicide for three successive days starting at 5 days after germination and resistant plants were maintained for subsequent analysis. T1 plants were screened for expression of desired constructs and two or three independent lines were carried on to the next generation for imaging. T2 seeds were bleach sterilized, plated on "MS plates, and cold-stratified at 4°C in the dark for 2 days before being moved to the grow room described above. Next, 5–7-day-old seedlings were then transplanted to soil and grown to flower for further analysis.

CLSM

All T1 lines were screened using a compound epifluorescence microscope (Nikon Eclipse Ni-U) with an X-Cite 120 LED fluorescent lamp and narrow-band eGFP and TXRed filter cubes. Mature flowers were selected and ovules dissected out retained on the septum and placed in PIPES buffer (50 mM PIPES, 5 mM EGTA and 1 mM $MgSO_4$ at pH 6.8) on a clean slide. Lines with varying levels of fluorescent marker accumulation were analyzed and carried forward to account for expression-level bias in marker distribution.

Final imaging was done in stable T2 lines using CLSM. Ovules were dissected out of emasculated flowers (after 2 days to ensure ovule maturity) and mounted in PIPES buffer on clean slides. Immediately after dissection, samples were imaged on a Leica TCS SP8 CLSM using a HC PL APO ×40 water immersion objective (NA = 1.10) with both GFP and cYFP excited using an argon laser (488 nm and 514 nm, respectively) and mCherry excited with a 561 nm diode laser in sequential mode. Fluorescence was detected differentially using two separate HyD detectors, both in photon counting mode, obtaining single sections of synergid cells at ×4.5 zoom.

Native promoter lines were imaged similar to above but with the following changes. Ovules from *LREpro*::*LRE–cYFP* in the *lre* mutant background and *NTApro*::*NTA–GFP* in Col-0 were imaged on the Leica TCS SP8 using a ×40 water immersion objective but with no zoom. Autofluorescence was detected simultaneously along with *LREpro*::*LRE–cYFP* using a 488 nm argon laser and a separate HyD detector. The *NTApro*::*NTA–GFP* ovule was counterstained and imaged along with FM464 (Molecular Probes, T3166) as in a previous study (Jones *et al.*, 2017).

Quantification of co-localization

Two-channel optical sections were cropped to include only the synergid cell and filtered to remove background noise and restrict data to the resolution limits of the microscope using a custom macro in Fiji (File S1) (Schindelin *et al.*, 2012). An initial median filter was used to remove salt-and-pepper detector noise. As the vesicles were near the limit of our optical resolution, we then took advantage of this and used a narrow-band spatial bandpass filter to remove background signal and instrument noise. Filtered datasets were then analyzed using the JACoP (Just Another Co-localization) plugin in Fiji (Bolte and Cordelieres, 2006). Distributions of MCC and PCC values were compared using the non-parametric Kruskal–Wallis test. Graphs and statistical analysis were performed using Graphpad Prism software (www.graphpad.com).

Image processing and figure construction

Micrographs were edited and analyzed using Fiji (Schindelin *et al.*, 2012). An ovule diagram was made using Inkscape v0.91 software. Figures were all constructed using Gimp v2.8.14 software.

ACKNOWLEDGEMENTS

We thank the Kessler and Palanivelu Laboratories for helpful discussions. This work was supported by National Science Foundation grants IOS-1733865 to S.A.K. and IOS-1146090 to R.P.

CONFLICT OF INTEREST

The authors have no conflicts of interest to declare.

CONTRIBUTIONS

D.S.J., X.L., R.P., S.A.K. designed experiments; D.S.J. and X.L. cloned constructs and generated plant lines; D.S.J. and A.C.W. imaged and analyzed the data; D.S.J and B.E.S performed the quantification analysis; D.S.J. and S.A.K. wrote the article.

SUPPORTING INFORMATION

Additional Supporting Information may be found in the online version of this article.

Figure S1. LRE–cYFP co-localization with Exo70E2 in the FA of mature synergids.

Table S1. Secretory markers analyzed in the Col-0 background.

Table S2. Number of synergids expressing TGN markers with FA localization vs. no FA localization.

Table S3. Secretory markers co-expressed and imaged with LRE and NTA.

Table S4. List of primers used for cloning secretory markers.

File S1. ImageJ macro for determination of degree of co-localization.

REFERENCES

Beale, K.M. and Johnson, M.A. (2013) Speed dating, rejection, and finding the perfect mate: advice from flowering plants. *Curr. Opin. Plant Biol.* **16**, 590–597.

Bent, A. (2006) *Arabidopsis thaliana Floral Dip Transformation Method. In Methods in Molecular Biology Wang*, K edn. Totowa, NJ: Humana Press Inc.

Bhat, R.A., Miklis, M., Schmelzer, E., Schulze-Lefert, P. and Panstruga, R. (2005) Recruitment and interaction dynamics of plant penetration resistance components in a plasma membrane microdomain. *Proc. Natl Acad. Sci. USA* **102**, 3135–3140.

Bolte, S. and Cordelieres, F. (2006) A guided tour into subcellular co-localization analysis in light microscopy. *J. Microsc.* **224**, 213–232.

Capron, A., Gourgues, M., Neiva, L.S., Faure, J.-E., Berger, F., Pagnussat, G., Krishnan, A., Alvarez-Mejia, C., Vielle-Calzada, J.-P. and Lee, Y.-R. (2008) Maternal control of male-gamete delivery in Arabidopsis involves a putative GPI-anchored protein encoded by the LORELEI gene. *Plant Cell*, **20**, 3038–3049.

Chevalier, É., Loubert-Hudon, A., Zimmerman, E.L. and Matton, D.P. (2011) Cell–cell communication and signalling pathways within the ovule: from its inception to fertilization. *New Phytol.* **192**, 13–28.

Dettmer, J., Hong-Hermesdorf, A., Stierhof, Y.-D. and Schumacher, K. (2006) Vacuolar H+-ATPase activity is required for endocytic and secretory trafficking in Arabidopsis. *Plant Cell*, **18**, 715–730.

Ding, Y., Wang, J., Wang, J., Stierhof, Y.-D., Robinson, D.G. and Jiang, L. (2012) Unconventional protein secretion. *Trends Plant Sci.* **17**, 606–615.

Ding, Y., Wang, J., Lai, J.H.C., Chan, V.H.L., Wang, X., Cai, Y., Tan, X., Bao, Y., Xia, J. and Robinson, D.G. (2014) Exo70E2 is essential for exocyst subunit recruitment and EXPO formation in both plants and animals. *Mol. Biol. Cell* **25**, 412–426.

Drakakaki, G. and Dandekar, A. (2013) Protein secretion: how many secretory routes does a plant cell have? *Plant Sci.* **203–204**, 74–78.

Drews, G.N. and Yadegari, R. (2002) Development and function of the angiosperm female gametophyte. *Annu. Rev. Genet.* **36**, 99–124.

Dunn, K.W., Kamocka, M.M. and McDonald, J.H. (2011) A practical guide to evaluating co-localization in biological microscopy. *Am. J. Physiol. Cell Physiol.* **300**, C723–C742.

Escobar-Restrepo, J.M., Huck, N., Kessler, S., Gagliardini, V., Gheyselinck, J., Yang, W.C. and Grossniklaus, U. (2007) The FERONIA receptor-like kinase mediates male-female interactions during pollen tube reception. *Science*, **317**, 656–660.

Foresti, O. and Denecke, J. (2008) Intermediate organelles of the plant secretory pathway: identity and function. *Traffic*, **9**, 1599–1612.

Geldner, N., Anders, N., Wolters, H., Keicher, J., Kornberger, W., Müller, P., Delbarre, A., Ueda, T., Nakano, A. and Jürgens, G. (2003) The Arabidopsis GNOM ARF-GEF mediates endosomal recycling, auxin transport, and auxin-dependent plant growth. *Cell*, **112**, 219–230.

Geldner, N., Dénervaud-Tendon, V., Hyman, D.L., Mayer, U., Stierhof, Y.D. and Chory, J. (2009) Rapid, combinatorial analysis of membrane compartments in intact plants with a multicolor marker set. *Plant J.* **59**, 169–178.

Gibson, D.G., Young, L., Chuang, R.-Y., Venter, J.C., Hutchison, C.A. and Smith, H.O. (2009) Enzymatic assembly of DNA molecules up to several hundred kilobases. *Nat. Methods*, **6**, 343–345.

Gunning, B.E.S. and Pate, J.S. (1969) 'Transfer cells' plant cells with wall ingrowths, specialized in relation to short distance transport of solutes – their occurrence, structure, and development. *Protoplasma*, **68**, 107–133.

Hafidh, S., Fíla, J. and Honys, D. (2016) Male gametophyte development and function in angiosperms: a general concept. *Plant Reprod.* **29**, 31–51.

Higashiyama, T. and Takeuchi, H. (2015) The mechanism and key molecules involved in pollen tube guidance. *Annu. Rev. Plant Biol.* **66**, 393–413.

Huang, B.-Q. and Russell, S.D. (1992) Female germ unit: organization. *Isol. Funct.* **140**, 233–293.

Hückelhoven, R. and Panstruga, R. (2011) Cell biology of the plant–powdery mildew interaction. *Curr. Opin. Plant Biol.* **14**, 738–746.

Jensen, W.A. (1965) The ultrastructure and histochemistry of the synergids of cotton. *Am. J. Bot.* **52**, 238–256.

Jones, D.S., Yuan, J., Smith, B.E., Willoughby, A.C., Kumimoto, E.L. and Kessler, S.A. (2017) MILDEW RESISTANCE LOCUS O function in pollen tube reception is linked to its oligomerization and subcellular distribution. *Plant Physiol.* **175**, 172–185.

Kessler, S.A. and Grossniklaus, U. (2011) She's the boss: signaling in pollen tube reception. *Curr. Opin. Plant Biol.* **14**, 622–627.

Kessler, S.A., Shimosato-Asano, H., Keinath, N.F., Wuest, S.E., Ingram, G., Panstruga, R. and Grossniklaus, U. (2010) Conserved molecular components for pollen tube reception and fungal invasion. *Science*, **330**, 968–971.

Leshem, Y., Johnson, C. and Sundaresan, V. (2013) Pollen tube entry into the synergid cell of Arabidopsis is observed at a site distinct from the filiform apparatus. *Plant Reprod.* **26**, 93–99.

Li, C., Yeh, F.L., Cheung, A.Y. *et al.* (2015) Glycosylphosphatidylinositol-anchored proteins as chaperones and co-receptors for FERONIA receptor kinase signaling in Arabidopsis. *Elife*, **4**, e06587.

Lindner, H., Kessler, S.A., Müller, L.M., Shimosato-Asano, H., Boisson-Dernier, A. and Grossniklaus, U. (2015) TURAN and EVAN mediate pollen tube reception in Arabidopsis synergids through protein glycosylation. *PLoS Biol.* **13**, e1002139.

Liu, X., Castro, C., Wang, Y., Noble, J., Ponvert, N., Bundy, M., Hoel, C., Shpak, E. and Palanivelu, R. (2016) The role of LORELEI in pollen tube reception at the interface of the synergid cell and pollen tube requires the modified eight-cysteine motif and the receptor-like kinase FERONIA. *Plant Cell*, **28**, 1035–1052.

Manders, E., Stap, J., Brakenhoff, G., Van Driel, R. and Aten, J. (1992) Dynamics of three-dimensional replication patterns during the S-phase, analysed by double labelling of DNA and confocal microscopy. *J. cell science.* **103**, 857–862.

Manders, E., Verbeek, F. and Aten, J. (1993) Measurement of co-localization of objects in dual-colour confocal images. *J. Microsc.* **169**, 375–382.

Mansfield, S.G., Briarty, L.G. and Erni, S. (1991) Early embryogenesis in *Arabidopsis thaliana*. I. The mature embryo sac. *Can. J. Bot.* **69**, 447–460.

Naramoto, S. (2017) Polar transport in plants mediated by membrane transporters: focus on mechanisms of polar auxin transport. *Curr. Opin. Plant Biol.* **40**, 8–14.

Nelson, B.K., Cai, X. and Nebenfuhr, A. (2007) A multicolored set of in vivo organelle markers for co-localization studies in Arabidopsis and other plants. *Plant J.* **51**, 1126–1136.

Okuda, S., Tsutsui, H., Shiina, K. *et al.* (2009) Defensin-like polypeptide LUREs are pollen tube attractants secreted from synergid cells. *Nature*, **458**, 357–361.

Reyes, F.C., Buono, R. and Otegui, M.S. (2011) Plant endosomal trafficking pathways. *Curr. Opin. Plant Biol.* **14**, 666–673.

Russell, S.D. (1992) Double fertilization. *Int. Rev. Cytol.* **140**, 357–388.

Rutherford, S. and Moore, I. (2002) The Arabidopsis Rab GTPase family: another enigma variation. *Curr. Opin. Plant Biol.* **5**, 518–528.

Samuel, M.A., Chong, Y.T., Haasen, K.E., Aldea-Brydges, M.G., Stone, S.L. and Goring, D.R. (2009) Cellular pathways regulating responses to compatible and self-incompatible pollen in Brassica and Arabidopsis stigmas intersect at Exo70A1, a putative component of the exocyst complex. *Plant Cell*, **21**, 2655–2671.

Sanderfoot, A.A., Kovaleva, V., Bassham, D.C. and Raikhel, N.V. (2001) Interactions between syntaxins identify at least five SNARE complexes within the Golgi/prevacuolar system of the Arabidopsis cell. *Mol. Biol. Cell*, **12**, 3733–3743.

Schindelin, J., Arganda-Carreras, I., Frise, E. *et al.* (2012) Fiji: an open-source platform for biological-image analysis. *Nat. Methods*, **9**, 676–682.

Sumner, M. and Caeseele, L.V. (1989) The ultrastructure and cytochemistry of the egg apparatus of *Brassica campestris*. *Can. J. Bot.* **67**, 177–190.

Takeuchi, H. and Higashiyama, T. (2012) A species-specific cluster of defensin-like genes encodes diffusible pollen tube attractants in Arabidopsis. *PLoS Biol.* **10**, e1001449.

Tian, G.-W., Mohanty, A., Chary, S.N., Li, S., Paap, B., Drakakaki, G., Kopec, C.D., Li, J., Ehrhardt, D. and Jackson, D. (2004) High-throughput fluorescent tagging of full-length Arabidopsis gene products in planta. *Plant Physiol.* **135**, 25–38.

Tsukamoto, T., Qin, Y., Huang, Y., Dunatunga, D. and Palanivelu, R. (2010) A role for LORELEI, a putative glycosylphosphatidylinositol-anchored protein, in Arabidopsis thaliana double fertilization and early seed development. *Plant J.* **62**, 571–588.

Tucker, M.R. and Koltunow, A.M. (2014) Traffic monitors at the cell periphery: the role of cell walls during early female reproductive cell differentiation in plants. *Curr. Opin. Plant Biol.* **17**, 137–145.

Viotti, C., Bubeck, J., Stierhof, Y.-D., Krebs, M., Langhans, M., van den Berg, W., van Dongen, W., Richter, S., Geldner, N. and Takano, J. (2010) Endocytic and secretory traffic in Arabidopsis merge in the trans-Golgi network/early endosome, an independent and highly dynamic organelle. *Plant Cell*, **22**, 1344–1357.

Wang, J., Ding, Y., Wang, J., Hillmer, S., Miao, Y., Lo, S.W., Wang, X., Robinson, D.G. and Jiang, L. (2010) EXPO, an exocyst-positive organelle distinct from multivesicular endosomes and autophagosomes, mediates cytosol to cell wall exocytosis in Arabidopsis and tobacco cells. *Plant Cell*, **22**, 4009–4030.